

Local Nonlinearity Dominates Directional Focused Extreme Waves in Intermediate Depth

Min Gao*, Paul H. Taylor, Hugh Wolgamot

School of Earth and Oceans, The University of Western Australia, Perth, Australia

E-mail: min.gao@uwa.edu.au

1 INTRODUCTION

Extreme crest events remain a primary driver of hydrodynamic loads and operational risk for offshore structures. In random seas, large crests can arise through linear dispersive focusing and constructive interference, but there is continuing discussion about how much nonlinear dynamics contribute to the formation and severity of such events under realistic storm conditions. In particular, mechanisms associated with envelope-scale (global) nonlinearity, often discussed in terms of Benjamin–Feir instability [1] and four-wave resonances [2], are theoretically capable of producing localised extremes in narrow-banded, nearly unidirectional deep water wave trains. Thus, the Peregrine breather in the NLS equation has a local peak of three times the regular wave background. However, the relevance of this pathway to real ocean sea states is uncertain because broader bandwidth, directional spreading, and finite water depth are all expected to weaken modulational growth. In contrast, second-order bound nonlinearities act primarily at the wave-shape level, producing crest sharpening, crest–trough asymmetry, and mean set-down beneath groups, thereby enhancing the severity of crest-scale kinematics without requiring substantial envelope growth.

Fully nonlinear simulations of directionally spread wave groups have previously shown a systematic, anisotropic reshaping of the focused packet, with contraction in the mean propagation direction and broadening laterally. In particular, Gibbs and Taylor (2005) [3] and Adcock et al. (2012) [4] reported this “wall of water” group evolution and attributed the dominant contribution to higher-order free-wave interactions, highlighting the role of the $\eta^{(3)}$ term in their decomposition. Building on these insights, the present work examines whether the same envelope deformation and strongly localised kinematics are present for NewWave-type focused groups representative of realistic storm sea states (with directional spreading and finite/intermediate depth) computed using a fully nonlinear solver. By comparing the nonlinear evolution with the corresponding linear focused simulation, we assess the extent to which the group envelope departs from linear dispersive focusing and examine the degree to which nonlinear effects manifest as localized crest-scale steepening and severe kinematics beneath the focused event.

2 WAVE MODELLING

A representative sea state from the North Sea was selected, characterised by a peak period of 15.3 s, a significant wave height of 12.8 m, and on a water depth of 92 m. The extreme event was represented by a focused wave group in the NewWave formulation, and a three-dimensional directionally spread NewWave form, following Barratt et al. [5] was adopted. The focused wave group simulated here is derived from the JONSWAP spectrum, which characterises the energy distribution of irregular sea states. The spectrum is defined by a peak frequency corresponding to the peak period of the selected representative sea state and a peak enhancement factor ($\gamma=2$) to capture the spectral peak sharpening. The linear amplitude of the spectrum is set equal to the significant wave height representing the characteristic energy level of the sea state. To avoid spurious high frequency components, the spectrum is truncated above 2.5 times the peak frequency.

Directional spreading is incorporated by extending the unidirectional JONSWAP spectrum $S(\omega)$ into a directional spectrum $F(\omega, \theta)$ expressed as $F(\omega, \theta) = S(\omega)D(\theta)$. Here, ω is the angular frequency, θ is the direction of wave propagation, and $D(\theta)$ is the spreading function. In this study, a frequency independent Gaussian spreading function, as adopted by Barratt et al. [5], is employed to model the directional spreading, ensuring a realistic representation of wave energy distribution across directions. The designed NewWave form at the linear focus time is illustrated in Figure 1.

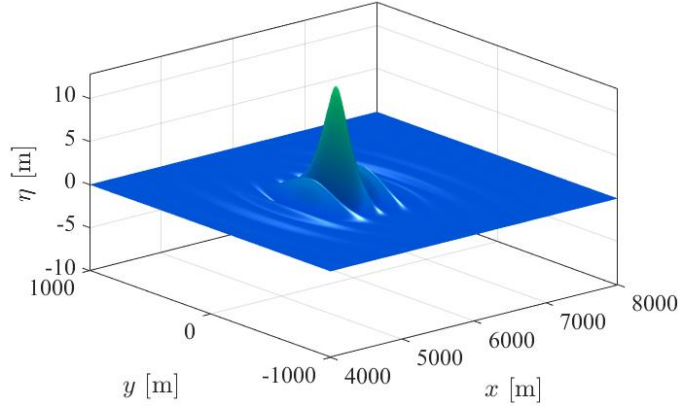


Figure 1: The 3D wave field of the designed NewWave-type focused wave group at the linear focus time, showing the wave crest at its maximum height.

Wave evolution was simulated using the nonlinear potential flow solver OceanWave3D, developed for the simulation of surface gravity waves in three-dimensional domains with variable bathymetry by Engsig-Harup et al. [6]. OceanWave3D has been widely used for simulating wave propagation, nonlinear interactions, and extreme wave events. Its ability to resolve third-order resonant interactions and accurate wave kinematics from the sea bed to the moving free surface makes it a robust tool for studying wave dynamics and assessing loads on offshore structures. Further detailed descriptions and additional methodological insights can be found in Engsig-Karup et al. [6] and Bingham and Zhang [7].

A rectangular numerical wave tank with dimensions 11520 m in length, 5120 m in width, and 92 m in depth was employed for the simulations. The grid resolution was selected based on the mesh convergence study by Barratt et al. [5] to ensure numerical accuracy. Accordingly, the 3D computational domain was discretized into $(N_x, N_y, N_z) = (2048, 512, 9)$ grid points. The boundary condition at the sidewalls is no flow normal to the boundary, enforced via a Neumann-type condition on the velocity potential. We prescribed initial conditions for the surface elevation and velocity potential at the free surface. The focused wave group was propagated backward linearly by 12 wave periods to construct the initial condition. The simulation is then advanced for approximately $16 T_p$, thereby concluding 4 periods after the linear focus event. This setup efficiently captures the focused event with adequate accuracy. A uniform phase shift of 90° , 180° , 270° has been applied to the initial condition to achieve another three focused wave groups with the waves at different points within the same wave envelope.

3 RESULTS

Figure 2(a) presents the free surface elevation time series at the location where the maximum crest occurs, obtained from the four phase-shifted simulations (0° , 90° , 180° , and 270°). All four runs exhibit a consistent focused wave group and reach a peak crest of approximately 15 m at the focus time. Relative to the assigned linear amplitude, this corresponds to a clear nonlinear crest enhancement at focus. To quantify the nonlinear content, the four-phase decomposition is applied to separate the first-order component and the higher-order bound harmonics. The resulting harmonic contributions are shown in Figure 2(b). The first-order elevation $\eta^{(1)}$ yields a crest amplitude of 12.18 m, slightly below the prescribed linear target (12.8 m), indicating a modest reduction in achieved linear focusing. In contrast, the sum-frequency second-order term $\eta^{(2+)}$ contributes about 2.5 m at the crest, with a further 1 m from the third-order component $\eta^{(3)}$ and a smaller 0.41 m fourth-order contribution $\eta^{(4)}$. These magnitudes confirm that the focused event is dominated by strong bound-harmonic (local) nonlinearity near focus.

Figure 3 compares the wave envelop in space of the focused wave group at the focus time $t = t_0$ from the fully nonlinear simulation with the corresponding linear dispersive NewWave simulation. The nonlinear case retains the same overall footprint and peak location with the linear run, indicating that the event remains a focused group rather than undergoing substantial envelope amplification. However, an underlying group

shape deformation is evident: the high-amplitude area becomes more compact in the mean wave direction x , while simultaneously expanding in the lateral direction y . This pattern is consistent with the shape

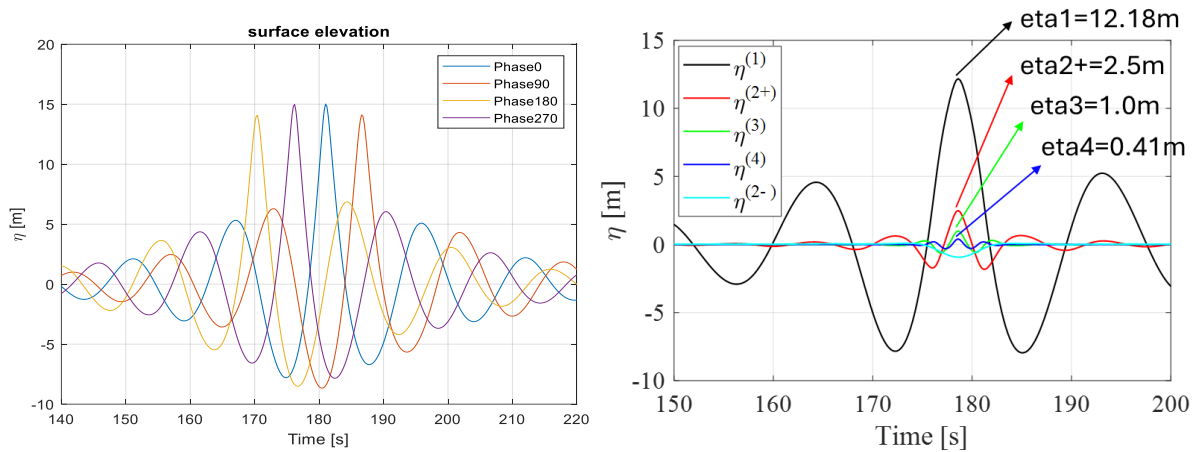


Figure 2: (a) Time series of the free surface elevation at the achieved focus location obtained from four phase-shifted simulations; (b) first and higher order harmonics separated from four-phase decomposition.

changes of a focussed wave group discussed in [3] and [4]. Unlike the Benjamin-Feir instability of regular uni-directional waves, there is no extra elevation at the centre of the group, but there is a slight contraction of the group along the mean wave direction and slight extension of the group laterally. Here, with a realistic bandwidth and directional spreading, these effects are rather minor. In addition to these subtle changes, the focussed group has locally large bound harmonics. This, our results can be viewed as consistent with both earlier fully nonlinear studies of directionally spread groups [3, 4] and the recent findings from the field measurements at the Ekofisk offshore platform in the central North Sea [8] which stressed the importance of the bound components.

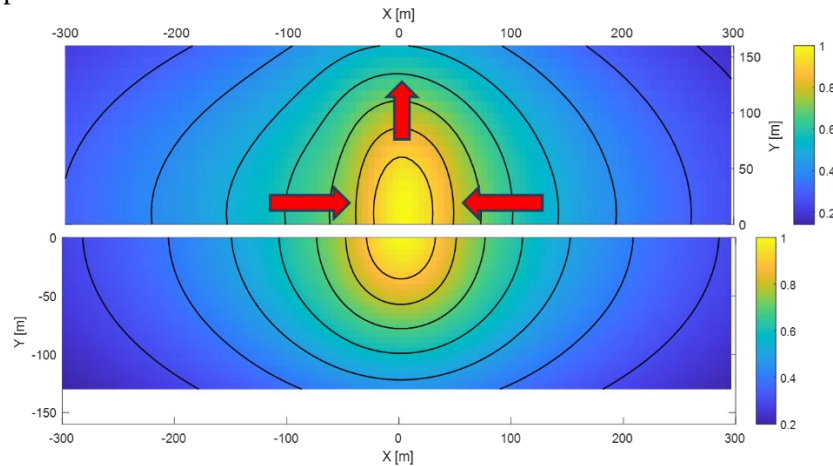


Figure 3: Wave envelope in space at the focus time from the fully nonlinear simulation (top half) and the linear dispersive run (bottom half)

Figure 4 presents the wave kinematics beneath the crest at the focus location for the Phase 0 case. Here, t_0 denotes the instant of maximum surface elevation, and velocity profiles are shown at $t_0 \pm 0.6\text{s}$ and $t_0 \pm 1.0\text{s}$ to illustrate the temporal evolution around the focused crest. In addition to the baseline case (target linear amplitude $A = 12.8\text{m}$), two higher amplitude cases ($A = 15\text{m}$ and 18m) are included; these generate nonlinear crest elevations of approximately 18 m and 22 m, respectively. Across all cases, the velocity profiles at t_0 exhibit severe near surface kinematics, indicating that the most severe flow occurs in a narrow time window centred on the peak crest. By contrast, profiles only 0.6–1.0 s before or after t_0 return rapidly toward milder conditions, despite the wave group still being present. This rapid decay away from t_0 becomes increasingly pronounced as the linear amplitude increases, demonstrating that the strongest nonlinear kinematics are highly localised in time and space.

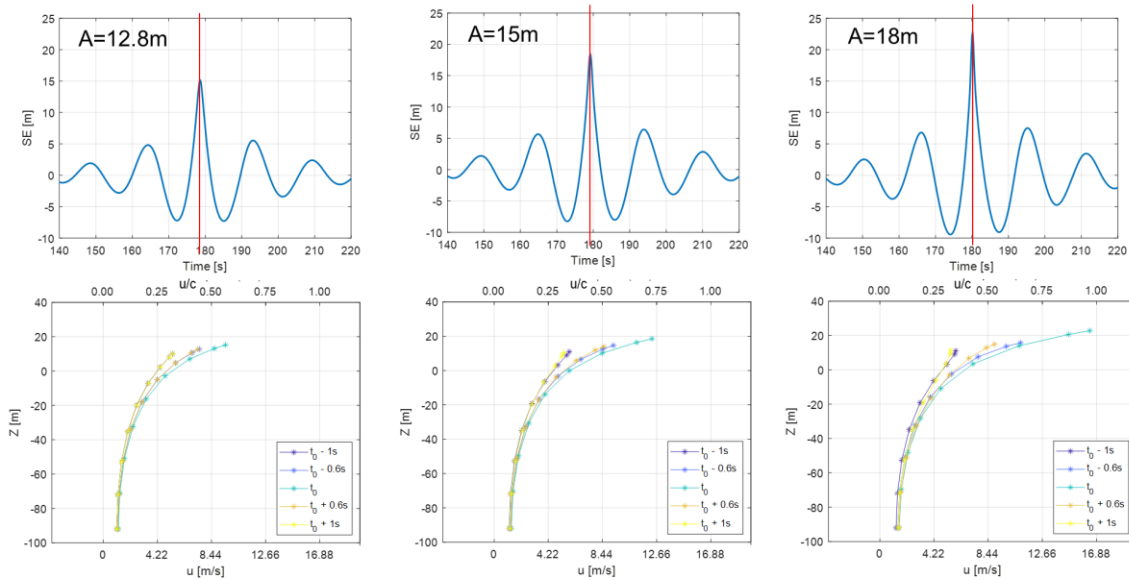


Figure 4: The profile of the focused crest and the wave kinematics beneath the crest from the focused wave group of three linear amplitude ($A=12.8\text{m}$, 15m , and 18m from left to right panel). The horizontal scale at the top of kinematics plot shows (u/c) where c is the linear phase speed for a wave of frequency f_p .

4 CONCLUSIONS

The fully nonlinear OceanWave3D simulations of 3D directionally spread NewWave type focused wave groups indicate that nonlinearity in these realistic storm-like conditions is primarily local rather than global. Compared with the corresponding linear run, the focused event retains a similar group-scale footprint, with only modest envelope reshaping, slight contraction in the mean wave direction and lateral broadening, consistent with bound-harmonic effects. The wave kinematics beneath the peak crest are exceptionally intense yet confined to a narrow time and space region. These results demonstrated that extreme crests arise mainly from linear dispersive focusing, with bound nonlinearities sharpening the crest and intensifying near surface kinematics.

ACKNOWLEDGEMENT

This research is supported by the Australian Research Council Industrial Transformation Research Hub for Transforming energy Infrastructure through Digital Engineering (TIDE, <http://TIDE.edu.au>). The support in resources provided by the Pawsey Supercomputing Centre with funding from the Australian Government and the Government of Western Australia is acknowledged. We thank Xinyu Liu and Tom Adcock of Oxford for the use of their code to specify 2nd-order accurate initial conditions for our OceanWaves3D runs.

REFERENCES

- [1] Benjamin, T.B. and Feir, J.E., 1967. The disintegration of wave trains on deep water Part 1. Theory. *Journal of Fluid Mechanics*, 27(3), pp.417-430.
- [2] Zakharov, V.E., 1968. Stability of periodic waves of finite amplitude on the surface of a deep fluid. *Journal of Applied Mechanics and Technical Physics*, 9(2), pp.190-194.
- [3] Gibbs, R.H. and Taylor, P.H., 2005. Formation of walls of water in ‘fully’ nonlinear simulations. *Applied Ocean Research*, 27(3), pp.142-157.
- [4] Adcock, T.A., Gibbs, R.H. and Taylor, P.H., 2012. The nonlinear evolution and approximate scaling of directionally spread wave groups on deep water. *Proceedings of the Royal Society A: Mathematical, Physical and Engineering Sciences*, 468(2145), pp.2704-2721.
- [5] Barratt, D., Bingham, H.B. and Adcock, T.A., 2020. Nonlinear evolution of a steep, focusing wave group in deep water simulated with OceanWave3D. *Journal of Offshore Mechanics and Arctic Engineering*, 142(2), p.021201.
- [6] Engsig-Karup, A.P., Bingham, H.B. and Lindberg, O., 2009. An efficient flexible-order model for 3D nonlinear water waves. *Journal of computational physics*, 228(6), pp.2100-2118.
- [7] Bingham, H.B. and Zhang, H., 2007. On the accuracy of finite-difference solutions for nonlinear water waves. *Journal of Engineering Mathematics*, 58, pp.211-228.
- [8] Knobler, S., Malila, M.P., Tayfun, M.A., Liberzon, D. and Fedele, F., 2025. Effects of bound-wave asymmetry on North Sea rogue waves. *Scientific Reports*, 15(1), p.20609.